

# Non-Markovian Quantum Error Deterrence by Dynamical Decoupling in a General Environment

K. Shiokawa <sup>\*</sup> and B. L. Hu <sup>†</sup>

Department of Physics, University of Maryland, College Park, MD 20742, USA

(July 13, 2005)

## Abstract

A dynamical decoupling scheme for the deterrence of errors in the non-Markovian (usually corresponding to low temperature, short time, and strong coupling) regimes suitable for qubits constructed out of a multilevel structure is studied. We use the effective spin-boson model (ESBM) introduced recently [K. Shiokawa and B. L. Hu, Phys. Rev. A 70, 062106 (2004)] as a low temperature limit of the quantum Brownian oscillator model, where one can obtain exact solutions for a general environment with colored noises. In our decoupling scheme a train of pairs of strong pulses are used to evolve the interaction Hamiltonian instantaneously. Using this scheme we show that the dynamical decoupling method can suppress  $1/f$  noise with slower and hence more accessible pulses than previously studied, but it still fails to decouple super-Ohmic types of environments.

---

<sup>\*</sup>E-mail address: kshiok@physics.umd.edu

<sup>†</sup>E-mail address: hub@physics.umd.edu

# 1 Introduction

In quantum information science, quantum coherence and entanglement are used as essential resources for efficient information processing. Since the interaction of a system with its environment can destruct the coherence and destroy the entanglement, it is regarded as the most serious obstacle in the realistic implementation of quantum information processing [1, 2, 3].

**Fast time low temperature strong field challenges** In our previous paper [4], we introduced an Effective Spin-Boson Model (ESBM), obtained as the low temperature limit of the quantum Brownian oscillator model (QBM) [5, 6] when the system behaves effectively like a two-level system. In the absence of external fields, the solutions of ESBM match with the exact solutions for the spin-boson model[7, 8]. At a finite temperature and in the presence of an external field, the multilevel structure inherent in ESBM provides a quantitative measure of the leakage from the two-level system by transitions to other levels. Although leakage is unavoidable in many realistic qubit systems, most theoretical models ignore it. It is either interpreted as the difference between the theoretical prediction and the observation or estimated phenomenologically by crude approximations such as invoking the Fermi Golden rule which makes the Markovian assumption which may contradict the existent conditions.

Our model based on exact solutions for QBM enables us to estimate leakage analytically and provides an essential tool for probing the multilevel coherent dynamics without invoking the conventional approximations such as Born, Born-Markov, rotating-wave approximations (RWA). It also provides a systematic method for studying the quantum coherence of the system behavior in the presence of arbitrary external pulses which is used in error correction schemes. The exact decoherence and Rabi-oscillations in Ohmic and super-Ohmic environment were studied in [4]. We emphasize that we don't invoke the Markov approximation which is likely to be unreliable in the presently studied qubit models operating at *low temperatures*. In order to study the *short time* dynamics under strong and fast pulses, RWA, obtained by ignoring the counter rotating terms averaged out at long times, is also not suitable. Our model does not depend on these approximations and can thus serve the special yet important purpose of analyzing the short time dynamics under strong external fields.

**Error Correction versus Deterrence** One of the proposed methods to remove errors from quantum computation architecture is the use of error correcting codes, which enable one to detect and correct errors after they have occurred[3]. By encoding qubits in a redundant way, we can detect errors from majority voting. Although this method works irrespective of the source of errors, actual coding requires many physical qubits including ancillas and its implementation is not practical at the present stage of solid state qubits. When the system-bath interaction occurs collectively, we can encode qubits in the decoherence free subspace in order to avoid decoherence before it occurs[9].

In this paper, we apply the ESBM to quantum error deterrence by dynamical decoupling,

in which the external pulses are used to overpower the influence of the environment on the system. Using the ESBM, we give a more systematic study of the decoupling method which hopefully provides deeper insights in these processes than previously done based on simpler models.

In the popular scheme known as “bang-bang” (BB) control one introduces a sequence of square pulses [10, 11, 12, 13, 14, 15, 16, 17, 18]. Most theoretical analysis of this method are directed at pure-dephasing in the spin-boson model: the system-bath interaction is through the Pauli matrix  $\sigma_z$ , or the atom-field interaction under the rotating wave approximation[15]. Similar techniques are used for the study of suppression of collisional decoherence [20] and spontaneous decay [19] or the modified coherent dynamics by applying sinusoidal waves[21].

Dynamical decoupling by spin-echo pulses has been commonly used to suppress decoherence due to magnetic field fluctuations for ion-trap quantum teleportation [22]. Similar to the spin-echo a pair of  $\pi$  pulses are used in the bang-bang control. In contrast, our decoupling method uses a rapid sequence of a pair of pulses with opposite sign to rotate the oscillator coordinate in the same direction in the phase space by mimicking the instantaneous Hamiltonian evolution. Since our ESBM model has more realistic features than those models previously used to study decoupling and the advantage of being exactly solvable, it provides an ideal testing ground for the effectiveness of dynamical decoupling in realistic settings beyond the regimes delimited by conventional approximations.

It has been argued that for the decoupling to be successful one needs to use fast pulses with pulse duration much shorter than the inverse frequency cutoff of the bath,

$$\Delta t \ll 1/\Lambda_{UV}, \quad (1)$$

[11]. In [23], it was shown that when dynamical decoupling is applied to  $1/f$  noise, or more generally,  $1/f^\alpha$  ( $\alpha > 0$ ), the pulses can be somewhat slower although the condition

$$\Delta t < \pi/\Lambda_{UV}, \quad (2)$$

still needs to be satisfied. The decoupling was shown to be more effective when the noise originates from a bath with  $1/f$  spectrum than in the Ohmic case due to infrared (IR) dominance of modes in the  $1/f$  spectrum.

Noise with  $1/f$  type of spectrum are ubiquitous and appears in a wide variety of circumstances, for instance, river flow, sunspot activity, neuronal spike trains, and human coordination[24]. Various interpretations are given but so far no explanation is universal. For electronic systems, it is often attributed to the motion of defects or impurities or background charge fluctuations, although different interpretations are possible.

In [28], an experiment was performed with spin-echo-type pulses to identify the dominant source of decoherence in superconducting charge qubits made of Cooper-pair boxes. The authors concluded that a dominant source of decoherence is due to  $1/f$  charge noise. In [23], the authors argued that similar techniques can be used to efficiently suppress the  $1/f$  noise. They also discussed the limitation and general applicability of decoupling pulses. Similar results were found in the study of bang-bang control against telegraph noise[25].

On a short time scale comparable to the bath time scale, the details of the system-bath interaction and internal bath dynamics are no longer negligible. Those details will emerge when non-Markovian features of the dynamics become important. For the QBM model, these details are captured by the bath spectral density  $I(\omega)$ . For  $1/f$  noise the spectral density is concentrated in the low frequency range. As a result, the decoupling result depends more sensitively on the lower than on the upper cutoff. For the pulse interval close to the threshold value, decoherence rate can increase[23] (see Eq. (4)). Similar accentuation of the decay process can occur from infrequent measurements, which is known as the quantum anti-Zeno effect[26].

In Sec. 2 we discuss the effect of a quantum Brownian harmonic oscillator (QBO) under the influence of a general environment and an external pulse field. We use the Fock space representation for the harmonic QBO to define an effective two level system. In Sec. 3 we introduce dynamical decoupling (DD) in this effective spin-boson model (ESBM) and describe how to design pulses to minimize the influence of the environment and limit the leakage (to higher levels). We describe how well our DD scheme work in error deterrence for different environments. In Sec. 4 we draw the conclusions.

## 2 Modified quantum Brownian motion due to pulses

### 2.1 The model

Our model consists of a quantum Brownian particle interacting with a thermal bath in the presence of external pulses. We use the units in which  $k_B = \hbar = 1$ . The Hamiltonian for our model can be written as

$$H = H_S + H_E + H_I + H_P, \quad (3)$$

where the dynamics of the system  $S$  (with coordinate  $x$  and momentum  $p$ ) is described by the Hamiltonian

$$H_S = \frac{p^2}{2M} + V(x). \quad (4)$$

The Hamiltonian of the environment is assumed to be composed of harmonic oscillators with natural frequencies  $\omega_n$  and masses  $m_n$ ,

$$H_E = \sum_{n=1}^N \left( \frac{p_n^2}{2m_n} + \frac{m_n \omega_n^2 q_n^2}{2} \right). \quad (5)$$

where  $(q_1, \dots, q_N, p_1, \dots, p_N)$  are the coordinates and their conjugate momenta. The interaction between the system  $S$  and the environment  $E$  is assumed to be bilinear,

$$H_I = x \sum_{n=1}^N c_n q_n, \quad (6)$$

where  $c_n$  is the coupling constant between the quantum Brownian oscillator (QBO) and the  $n$ th environment oscillator with coordinate  $q_n$ . The coupling constants enter in the spectral density function  $I(\omega)$  of the environment defined by,

$$I(\omega) \equiv \pi \sum_n \frac{c_n^2}{2m_n\omega_n} \delta(\omega - \omega_n). \quad (7)$$

We assume the spectral density has the form

$$I(\omega) = 2M\gamma\omega^\nu e^{-\omega/\Lambda_{UV}}, \quad (8)$$

where  $\nu = 1$  is Ohmic,  $\nu < 1$  is sub-Ohmic, and  $\nu > 1$  is supra-Ohmic. We will study Ohmic, super-Ohmic with  $\nu = 3$ , and sub-Ohmic with  $1/f$  type noise. Since the last case is sensitive to the infrared (IR) regime, we introduce an infrared (IR) cutoff  $\Lambda_{IR}$  for our frequency integral. The law of large numbers tells us that a general environment consisting of a large number of fluctuators weakly coupled to the system can also be reduced to a bosonic environment. This description is supported numerically[27] and has been applied successfully to explain the effect of  $1/f$  noise on superconducting charge qubits[28].

For a linear QBO, the potential is

$$V(x) = \frac{M\Omega^2 x^2}{2}, \quad (9)$$

where  $\Omega$  is the natural frequency of the system oscillator. The pulse Hamiltonian has the form

$$H_P = H_S \sum_{n=1}^N P_n(t) \quad (10)$$

where

$$P_n(t) = \begin{cases} V & \Delta t \leq t < \Delta t + \tau \quad (\text{mod } 2\Delta t + 2\tau) \\ -V & -\tau \leq t < 0 \quad (\text{mod } 2\Delta t + 2\tau) \\ 0 & \text{otherwise} \end{cases}$$

Thus  $\tau$  is the duration of the pulse and  $\Delta t$  is the pulse interval between the end of one pulse and the beginning of another of opposite sign.

## 2.2 The influence functional of a system acted on by pulses

Here we will make connection with prior treatments of QBM based on the influence functional[5] with a phase space representation for the Wigner function[30]. First we define the transition amplitude between the initial state  $|x_0 q_0\rangle$  at  $t = 0$  and the final state  $|x q\rangle$  at time  $t$  to be

$$K(x, q; t | x_0, q_0; 0) \equiv \langle x q | U(t, 0) | x_0 q_0 \rangle. \quad (11)$$

where  $U(t, 0) = e^{-iHt}$  is a time evolution operator. In the presence of strong pulses, i.e.  $V \rightarrow \infty$  while keeping  $V\tau$  fixed, the pulse Hamiltonian commutes with the system-environment evolution Hamiltonian. Then the total amplitude can be sequenced in time as

$$K(x, q; t | x_0, q_0; 0) = \langle x | q | U(t, t_{2N}) U_p^\dagger U(t_{2N}, t_{2N-1}) U_p U(t_{2N-1}, t_{2N-2}) \dots U_p^\dagger U(t_2, t_1) U_p U(t_1, 0) | x_0 | q_0 \rangle \quad (12)$$

$$= \langle x | q | U(t, t_{2N}) U_p(t_{2N}, t_{2N-1}) U(t_{2N-1}, t_{2N-2}) \dots U_p(t_2, t_1) U(t_1, 0) | x_0 | q_0 \rangle \quad (13)$$

where  $U_p \equiv e^{-iH_S V \tau}$  and  $U_p(t_{2N}, t_{2N-1}) = e^{iH_S V \tau} U(t_{2N}, t_{2N-1}) e^{-iH_S V \tau}$  is the modified evolution kernel due to pulses. This form shows that the effect of a pair of pulses is to evolve the system variable  $x$  in the interaction Hamiltonian *instantaneously* to  $x \cos(\Omega V \tau) + p \sin(\Omega V \tau) / \Omega$ . In phase space, this corresponds to an instantaneous rotation by an angle  $\Omega V \tau$ .

The Liouville equation for the density matrix is

$$i \frac{\partial}{\partial t} \rho(t) = [H, \rho(t)], \quad (14)$$

where  $[\cdot, \cdot]$  is the commutator. In the coordinate representation, the density matrix becomes

$$\rho(x, x', q, q', t) \equiv \langle x | q | \rho(t) | x' | q' \rangle \quad (15)$$

where we have used  $q \equiv \{q_n\}$  to denote the environment variables collectively. The time evolution of the density matrix is given by

$$\rho(x, x', q, q', t) = \int dx_0 dx'_0 dq_0 dq'_0 K(x, q; t | x_0, q_0; 0) \rho(x_0, x'_0, q_0, q'_0, 0) K^*(x', q'; t | x'_0, q'_0; 0). \quad (16)$$

For a factorized initial condition between the system and the environment:  $\rho(x_0, x'_0, q_0, q'_0, 0) = \rho_S(x_0, x'_0, 0) \otimes \rho_B(q_0, q'_0, 0)$ , after tracing out the environment harmonic oscillator variables, we obtain an equation for the reduced density matrix:

$$\rho_r(x, x', t) \equiv \int dq \rho(x, x', q, q, t) = \int dx_0 dx'_0 J_r(x, x'; t | x_0, x'_0; 0) \rho_S(x_0, x'_0, 0), \quad (17)$$

where its time evolution operator is given by

$$J_r(x, x'; t | x_0, x'_0; 0) = \int dq dq_0 dq'_0 K(x, q; t | x_0, q_0; 0) \rho_B(q_0, q'_0, 0) K^*(x', q; t | x'_0, q'_0; 0). \quad (18)$$

The total action of the system  $\mathcal{S}[x, x']$  enters as

$$J_r(x, x'; t | x_0, x'_0; 0) \equiv \int_{(x_0 x'_0)}^{(x x')} \mathcal{D}x \mathcal{D}x' e^{i\mathcal{S}[x, x']} \quad (19)$$

and consists of two contributions:

$$\mathcal{S}[x, x'] = \mathcal{S}_S[x, x'] + \mathcal{S}_{IF}[x, x']. \quad (20)$$

The action for the system  $\mathcal{S}_S$  is given by

$$\mathcal{S}_S = \int_0^t ds \{M\dot{R}(s)\dot{r}(s) - M\Omega^2 R(s)r(s)\}, \quad (21)$$

where  $R \equiv (x + x')/2$ ,  $r \equiv x - x'$ . The influence action  $\mathcal{S}_{IF}[x, x']$  accounts for the effect of the environment on the system  $S$  and is given by

$$\begin{aligned} \mathcal{S}_{IF}[R, r] = & i \int_0^t ds \int_0^s ds' y(s) \nu(s - s') y(s') \\ & - 2 \int_0^t ds \int_0^s ds' y(s) \mu(s - s') Y(s'), \end{aligned} \quad (22)$$

where  $Y(t) \equiv (x(t) + x'(t)) \cos \theta(t)/2 + M(\dot{x}(t) + \dot{x}'(t)) \sin \theta(t)/2\Omega$ ,  $y(t) \equiv (x(t) - x'(t)) \cos \theta(t) + M(\dot{x}(t) - \dot{x}'(t)) \sin \theta(t)\Omega$ . The time dependent angle  $\theta(t)$  is defined as

$$\theta(t) = \begin{cases} 0 & \Delta t \leq t < 2\Delta t \pmod{2\Delta t} \\ \Omega V \tau & -\Delta t \leq t < 0 \pmod{2\Delta t} \end{cases} \quad (23)$$

and

$$\mu(t) = -\frac{1}{\pi} \int_0^\infty d\omega I(\omega) \sin \omega t \quad (24)$$

$$\nu(t) = \frac{1}{\pi} \int_0^\infty d\omega I(\omega) \coth \frac{\beta\omega}{2} \cos \omega t, \quad (25)$$

are the dissipation and noise kernels respectively for an environment initially at thermal equilibrium. We are particularly interested in the case in which each pair of pulses rotate the system by an angle  $\pi$  in the phase space, i.e.,  $\Omega V \tau = (2n + 1)\pi$  with an integer  $n$ . In this special case, due to the periodic nature of the harmonic motion, difference between our method and the bang-bang control is reduced to the phase factor. The effect of these pulses is to modify the form of the influence kernels in the action to

$$\begin{aligned} \mathcal{S}_{IF}[R, r] = & i \int_0^t ds \int_0^s ds' r(s) \tilde{\nu}(s, s') r(s') \\ & - 2 \int_0^t ds \int_0^s ds' r(s) \tilde{\mu}(s, s') R(s'), \end{aligned} \quad (26)$$

where the modified kernels  $\tilde{\mu}$  and  $\tilde{\nu}$  are defined as

$$\tilde{\mu}(s, s') = \cos \theta(s) \mu(s - s') \cos \theta(s') \quad (27)$$

$$\tilde{\nu}(s, s') = \cos \theta(s) \nu(s - s') \cos \theta(s') \quad (28)$$

From Eqs. (26) the Euler-Lagrange equations for  $R$  and  $r$  are

$$M\ddot{R}(t) + M\Omega^2 R(t) + 2 \int_0^t ds \tilde{\mu}(t-s)R(s) = 0, \quad (29)$$

$$M\ddot{r}(t) + M\Omega^2 r(t) - 2 \int_s^t ds' \tilde{\mu}(t-s)r(s) = 0. \quad (30)$$

The effect of the environment is included in the nonlocal kernels  $\mu$  and  $\nu$ . On the other hand, these kernels contain the information of the past history of the environment as modified by the presence of the system variables. Thus these equations respect the self-consistency in the dynamics between the system and the environment.

If we formally write the two independent solutions of the homogeneous parts of Eq. (29) and Eq. (30) to be  $u_i(s)$  and  $v_i(s)$ ,  $i = 1, 2$ , with boundary conditions  $u_1(0) = 1, u_1(t) = 0, u_2(0) = 0, u_2(t) = 1$  and  $v_1(0) = 1, v_1(t) = 0, v_2(0) = 0, v_2(t) = 1$ , respectively, the solutions of these uncoupled equations can be specified uniquely by the initial and final conditions  $(R_0, R_t)$  and  $(r_0, r_t)$  as

$$\begin{aligned} R_c(s) &= R_0 u_1(s) + R_t u_2(s), \\ r_c(s) &= r_0 v_1(s) + r_t v_2(s). \end{aligned} \quad (31)$$

An evaluation of the path integral can be carried out which is dominated by the classical solutions in (31). With these classical solutions, we write the action  $\mathcal{S}[x, x']$  as

$$\begin{aligned} \mathcal{S}[R_c, r_c] &= (M\dot{u}_1(t)R_0 + M\dot{u}_2(t)R_t)r_t \\ &- (M\dot{u}_1(0)R_0 + M\dot{u}_2(0)R_t)r_0 \\ &+ i(a_{11}(t)r_0^2 + (a_{12}(t) + a_{21}(t))r_0 r_t + a_{22}(t)r_t^2). \end{aligned} \quad (32)$$

where

$$a_{kl}(t) = \frac{1}{2} \int_0^t ds \int_0^t ds' v_k(s) \tilde{\mu}(s-s') v_l(s') \quad (33)$$

(for  $k, l = 1, 2$ ) contains the effects on the system dynamics from fluctuations in the environment modified by the pulses.

Using the results above,  $J_r$  in Eq. (19) can be written in a compact form,

$$J_r(R_t, r_t; t | R_0, r_0; 0) = N(t) e^{i\mathbf{R}^T \mathbf{u} \mathbf{r} - \mathbf{r}^T \mathbf{a} \mathbf{r}}, \quad (34)$$

where  $(\mathbf{a})_{ij} = a_{ij}$ ,  $\mathbf{R}^T = (R_0, R_t)$  and  $\mathbf{r}^T = (r_0, r_t)$

$$\mathbf{u} = \begin{pmatrix} u_{11} & u_{12} \\ u_{21} & u_{22} \end{pmatrix} \equiv M \begin{pmatrix} -\dot{u}_1(0) & \dot{u}_1(t) \\ -\dot{u}_2(0) & \dot{u}_2(t) \end{pmatrix}. \quad (35)$$



### 2.3 QBM in the phase space representation

Formally the Wigner distribution function is related to the density matrix by

$$W(R, P, t) = \frac{1}{2\pi} \int dr e^{-iPr} \rho_r(R + r/2, R - r/2, t). \quad (36)$$

It obeys the evolution equation

$$W(R_t, P_t, t) = \int dR_0 dP_0 K(R_t, P_t; t | R_0, P_0; 0) W(R_0, P_0, 0), \quad (37)$$

where  $K(R, P; t | R_0, P_0; 0)$  is the propagator for the Wigner function defined by

$$K(R, P; t | R_0, P_0; 0) = \frac{1}{2\pi} \int dr dr_0 e^{-i(Pr - P_0 r_0)} J_r(R, r; t | R_0, r_0; 0). \quad (38)$$

It is given by

$$\begin{aligned} K(R, P; t | R_0, P_0; 0) &= \frac{N(t)}{2\pi} \int dr dr_0 e^{i(-Pr + P_0 r_0 + \mathcal{L})} \\ &= N_W(t) \exp \left[ -\delta \vec{X}^T \mathbf{\Sigma}^{-1} \delta \vec{X} \right], \end{aligned}$$

where  $N_W(t) = N(t)/2\sqrt{|\mathbf{a}|}$  and  $|\mathbf{a}|$  is the determinant of  $\mathbf{a}$ . The vector  $\delta \vec{X} = \vec{X} - \langle \vec{X} \rangle$ , with

$$\vec{X} = \begin{pmatrix} R \\ P \end{pmatrix}, \quad (39)$$

and

$$\langle \vec{X} \rangle = \begin{pmatrix} \langle R \rangle \\ \langle P \rangle \end{pmatrix} = \begin{pmatrix} C_{11} & C_{21} \\ C_{12} & C_{22} \end{pmatrix} \begin{pmatrix} R_0 \\ P_0 \end{pmatrix} = \frac{-1}{u_{21}} \begin{pmatrix} u_{11} & 1 \\ |\mathbf{u}| & u_{22} \end{pmatrix} \begin{pmatrix} R_0 \\ P_0 \end{pmatrix}. \quad (40)$$

Here  $\mathbf{\Sigma}$  is a matrix characterizing the induced fluctuations in the system from the influence of the environment:

$$\mathbf{\Sigma} = \frac{2}{u_{21}^2} \begin{pmatrix} a_{11} & a_{12}u_{21} - a_{11}u_{22} \\ a_{12}u_{21} - a_{11}u_{22} & a_{11}u_{22}^2 - 2a_{12}u_{21}u_{22} + a_{22}u_{21}^2 \end{pmatrix}. \quad (41)$$

Although many equivalent phase space representations are known[31], for our purpose, it is convenient to define the characteristic functions obtained by the Fourier transform of the phase space distribution functions as follows:

$$\chi_Q(z, \bar{z}, t) = \int d^2\alpha Q(\alpha, \bar{\alpha}) e^{i\bar{z}\bar{\alpha}} e^{iz\alpha} \quad (42)$$

$$\chi_W(z, \bar{z}, t) = \int d^2\alpha W(\alpha, \bar{\alpha}) e^{i\bar{z}\bar{\alpha}} e^{iz\alpha}, \quad (43)$$

where  $\alpha \equiv \sqrt{\Omega/2}R + i\sqrt{1/2\Omega}P$ . The characteristic function  $\chi_Q(z, \bar{z})$  for the Q-distribution is related to  $\chi_W(z, \bar{z})$ , the characteristic function for the Wigner distribution, as

$$\chi_Q(z, \bar{z}, t) = e^{-\frac{|z|^2}{2}} \chi_W(z, \bar{z}, t). \quad (44)$$

For instance, the characteristic function  $\chi_Q(z, \bar{z}, t)$  for the harmonic QBO evolved from the initial ground state has the following Gaussian form:

$$\chi_Q(z, \bar{z}, t) = \exp \left[ -\frac{\langle a^2(t) \rangle}{2} z^2 - \frac{\langle a^{\dagger 2}(t) \rangle}{2} \bar{z}^2 - \langle a(t)a^\dagger(t) \rangle |z|^2 \right]. \quad (45)$$

The time dependent coefficients are anti-normal ordered operator averages of second moments given by  $\langle a^2 \rangle = c + \sigma$ ,  $\langle aa^\dagger \rangle = C + \Sigma + 1/4$ , which have their origins in the classical trajectory  $\mathbf{C}$  of a damped harmonic oscillator in Eq. (40), the induced fluctuations  $\Sigma$  from the environment in Eq.(41). The relations of these components can be written as follows:

$$\begin{aligned} 8c &= C_{22}^2 - C_{11}^2 + \Omega^2 C_{12}^2 - \frac{C_{21}^2}{\Omega^2} + 2i(C_{11}C_{12} + C_{21}C_{22}) \\ 8C &= C_{11}^2 + \Omega^2 C_{12}^2 + \frac{C_{21}^2}{\Omega^2} + C_{22}^2 \\ 4\sigma &= \Omega \Sigma_{11} - \frac{\Sigma_{22}}{\Omega} + 2i\Sigma_{12} \\ 4\Sigma &= \Omega \Sigma_{11} + \frac{\Sigma_{22}}{\Omega} \end{aligned} \quad (46)$$

## 2.4 Fock states/phase space correspondence

The harmonic QBM

$$H_S^{(\infty)} + H_I^{(\infty)} = \Omega a^\dagger a + \sqrt{2\Omega} (a + a^\dagger) \sum_{n=1}^{N_B} c_n q_n \quad (47)$$

can be viewed as a limiting case of a finite  $N$ -level system:

$$H_S^{(N)} + H_I^{(N)} = \Omega S_N^+ S_N^- + (S_N^- + S_N^+) \Gamma_B \quad (48)$$

where  $N \rightarrow \infty$ . Here  $\Gamma_B \equiv \sum_{n=1}^{N_B} \tilde{c}_n q_n$  and we have absorbed the factor  $\sqrt{2\Omega}$  by defining  $\tilde{c}_n = \sqrt{2\Omega} c_n$ .  $S_N^-$  is a number lowering operator whose matrix element is  $(S_N^-)_{ij} \equiv \sqrt{i} \delta_{i+1,j}$  and its conjugate  $S_N^+$  is a number raising operator.

The correspondence between the Fock state representation for the pseudo spin qubits and the phase space representation of a density matrix is given by

$$\rho_{kl}(t) = \int \frac{d^2 z}{\pi} \chi_Q(z, \bar{z}, t) \langle k | e^{-i\bar{z}a^\dagger} e^{-iza} | l \rangle. \quad (49)$$

From Eq. (49) we can directly evaluate the density matrix in the Fock representation for an arbitrary quantum number. The Pauli spin representation from the lowest two level Fock representation are obtained as

$$\begin{aligned}\langle\sigma_x(t)\rangle &= \rho_{01}(t) + \rho_{10}(t) \\ \langle\sigma_y(t)\rangle &= i\rho_{10}(t) - i\rho_{01}(t) \\ \langle\sigma_z(t)\rangle &= \rho_{11}(t) - \rho_{00}(t).\end{aligned}\tag{50}$$

In [4], we explained in some detail the level reduction mechanism and the relation between ESBM and other models of quantum computing. Various models used in the study of quantum computation can be obtained from our ESBM in different limits.

At a finite temperature  $T$ , only modes in the harmonic oscillator up to  $N \sim k_B T / \hbar \Omega$  are excited. At sufficiently low temperature  $k_B T \sim \hbar \Omega$ , the effective excitable number of levels of a harmonic QBO is significantly reduced. In particular, at  $k_B T < \hbar \Omega$ , we expect that the system is effectively reduced to two-levels. In this limit, our system and interaction Hamiltonians are reduced to those of the spin-boson model

$$H_S^{(2)} + H_I^{(2)} = \Omega(S_2^z + \frac{1}{2}) + S_2^x \Gamma_B.\tag{51}$$

Simplified model of decoherence with a pure dephasing term[29] can be obtained as an adiabatic limit of ESBM when the Brownian oscillator is frozen, i.e.  $\Omega \rightarrow 0$  with an unitary change of basis. This model is suitable for the study of short time dynamics but it overestimates the decoherence as we will see in the next section. Dissipative system-bath coupling without counter rotating terms common in many quantum optics texts[31] is obtained by imposing a rotating wave approximation (RWA) on ESBM.

$$H_S + H_{SB} = \Omega S_2^+ S_2^- + (S_2^- + S_2^+) \Gamma_B \rightarrow H_S + H_{RWA} = \Omega S_2^+ S_2^- + \sum_{n=1}^{N_B} \tilde{c}_n (S_2^- b_n^\dagger + S_2^+ b_n),\tag{52}$$

where  $b_n = (\omega_n q_n + i p_n) / \sqrt{2\omega_n}$  are bath annihilation operators. The dynamics under this approximation cannot capture the fast dynamics at time scales less than the natural time scale of the system. Thus it is inadequate in the study of generic environments.

More generally, one can split the components of  $S_N^+ S_N^-$  as  $S_2^+ S_2^- + S_{N-2}^+ S_{N-2}^-$ , where  $S_{N-2}^\pm$  are raising and lowering operators acting on the space outside of the lowest two levels. Similarly,  $S_N^+ + S_N^- = S_2^+ + S_2^- + S_{N-2}^+ + S_{N-2}^- = S_2^x + S_{N-2}^x + T_{2,N-2}$ , where  $S_{N-2}^x$  acts only on the space outside of the lowest two levels and  $(T_{2,N-2})_{nm} = \sqrt{2} \delta_{n2} \delta_{m3}$  mixes the two sectors (inside and outside of the lowest two levels) and is thus responsible for the leakage.

## 3 Dynamical Decoupling

### 3.1 General Scheme

Quantum error correction based on coding schemes requires many physical qubits to encode information[3]. In more realistic situations where only a few physical qubits are available, the

implementation of quantum information processing (QIP) requires more practical methods to prevent decoherence. This is similar to the refocusing techniques frequently used in NMR, where a sequence of pulses is used to modify the influence of environment on the system. In the bang-bang control scheme, a rapid sequence of a pair of  $\pi$  pulses is used to reduce the effect of decoherence. In the scheme described in Sec. 2, a train of a pair of pulses with opposite signs to change the influence of the environment on the system.

**Pulses to diminish environmental influence** In order to successfully diminish the effect of the environment on the system we require the pulses to satisfy the following requirements: First, the pulses are assumed to be strong enough so that we can ignore  $H_S$  during the pulse operation compared to  $H_P$ . In this strong pulse limit while keeping  $\Omega V \tau = (2l + 1)\pi$  ( $l = 0, 1, 2, \dots$ ) fixed, we obtain  $e^{iH_P \tau} H_I e^{-iH_P \tau} = -H_I$ . Second, the pulses are assumed to be acting at sufficiently short intervals  $\Delta t$ . Once these conditions are satisfied, the repeated application of pulses will change the whole system evolution to

$$\begin{aligned}
U(t = 2\mathcal{N}\Delta t) &= \left[ e^{iH_P \tau} e^{-i\Delta t(H_S + H_E + H_I)} e^{-iH_P \tau} e^{-i\Delta t(H_S + H_E + H_I)} \right]^{\mathcal{N}} \\
&= e^{-i\Delta t(H_S + H_E - H_I)} e^{-i\Delta t(H_S + H_E + H_I)} \dots \\
&\quad e^{-i\Delta t(H_S + H_E - H_I)} e^{-i\Delta t(H_S + H_E + H_I)} \\
&\rightarrow e^{-it(H_S + H_E)}
\end{aligned} \tag{53}$$

where the limit with vanishing pulse intervals is taken:  $\Delta t \rightarrow 0, \mathcal{N} \rightarrow \infty$ , while  $t = 2\mathcal{N}\Delta t$  is kept fixed. Thus under these conditions, the effect of the environment can be successfully eliminated.

Note that the complete elimination of the environment is achieved only in the idealized limit  $\Delta t \rightarrow 0$ . In practice, it seems sufficient to add pulses faster than the environment characteristic scale such that the environment is effectively frozen in the duration of the pulses. It has been argued that this condition requires  $\Delta t \ll 1/\Lambda_{UV}$ [11], which is already too stringent for the known practical implementations. Thus it is worth examining whether this condition  $\Delta t \ll 1/\Lambda_{UV}$  is strictly necessary. It is also important to see from our pulse Hamiltonian (11) that the total energy will be unchanged from our pulse operations.

**Pulses to minimize leakage** In a multilevel system if we are only interested in limiting the leakage (see previous section) from the two lowest levels to the higher levels, we can shape the pulses to realize the decoupling operator[18]

$$U_D = e^{i\phi} \begin{pmatrix} -I_{(N-2) \times (N-2)} & 0 \\ 0 & I_{2 \times 2} \end{pmatrix}, \tag{54}$$

where  $\phi$  is a phase factor. The condition  $\{U_D, T_{2,N-2}\} = 0$  together with  $[U_D, H_S] = [U_D, H_E] = [U_D, S_2^x] = [U_D, S_{N-2}^x] = 0$  yields

$$U(t = 2\mathcal{N}\Delta t) = \left[ U_D^\dagger e^{-i\Delta t \{H_S + H_E + (S_2^x + S_{N-2}^x + T_{2,N-2})\Gamma_B\}} U_D e^{-i\Delta t \{H_S + H_E + (S_2^x + S_{N-2}^x + T_{2,N-2})\Gamma_B\}} \right]^{\mathcal{N}}$$

$$\begin{aligned}
&= e^{-i\Delta t\{H_S+H_E+(S_2^x+S_{N-2}^x-T_{2,N-2})\Gamma_B\}} e^{-i\Delta t\{H_S+H_E+(S_2^x+S_{N-2}^x+T_{2,N-2})\Gamma_B\}} \dots \\
&\quad e^{-i\Delta t\{H_S+H_E+(S_2^x+S_{N-2}^x-T_{2,N-2})\Gamma_B\}} e^{-i\Delta t\{H_S+H_E+(S_2^x+S_{N-2}^x+T_{2,N-2})\Gamma_B\}} \\
&\rightarrow e^{-it\{H_S+H_E+(S_2^x+S_{N-2}^x)\Gamma_B\}}
\end{aligned} \tag{55}$$

where the limit with vanishing pulse intervals is taken:  $\Delta t \rightarrow 0, \mathcal{N} \rightarrow \infty$ , while  $t = 2\mathcal{N}\Delta t$  is kept fixed. The leakage can be eliminated in this limit. This method, however, will not change the coherence property within the computational Hilbert space. Thus decoherence within such space is not preventable with this method. We now discuss the dynamical decoupling scheme which protects the computational Hilbert space from the influence of the environment.

### 3.2 Dynamical Decoupling in QBM: Quantum Control of the Uncertainty Relation

We detour a bit here to show how dynamical decoupling can alter the uncertainty relation in quantum mechanics. The uncertainty principle [32] is a basic requirement for any quantum states to satisfy. In an open quantum system, information in the system is partly lost to the environment, resulting in a greater uncertainty in the quantum states of the open system than in the original closed system. The modified uncertainty relation in QBM in Ohmic environment has been studied before[6]. Here we study the uncertainty relation in general environment. A suitable measure for the uncertainty of an open quantum system is

$$A^2 \equiv (\Delta R)^2(\Delta P)^2 - \frac{1}{4}\{\langle \Delta R, \Delta P \rangle\}^2. \tag{56}$$

The uncertainty principle for open systems requires that for any physical state (pure or mixed, equilibrium or nonequilibrium) should satisfy  $A \geq 1/2$ .

Using the identity

$$\langle aa^\dagger \rangle^2 - \langle a^2 \rangle \langle a^{\dagger 2} \rangle = A^2 + \frac{\langle R^2 \rangle}{2} + \frac{\langle P^2 \rangle}{2} + \frac{1}{4} \tag{57}$$

and  $\langle R^2 \rangle + \langle P^2 \rangle \geq 1$  from the usual uncertainty principle, we obtain  $\langle aa^\dagger \rangle^2 - \langle a^2 \rangle \langle a^{\dagger 2} \rangle \geq 1$ . Combining this with (45) and (49) yields the ground state population  $\rho_{00} = (\langle aa^\dagger \rangle^2 - \langle a^2 \rangle \langle a^{\dagger 2} \rangle)^{-1/2} \leq 1$ . This can also be inferred directly from a probability requirement. From our Fock state/phase space correspondence in (49), we can reconstruct the temporal phase space uncertainty relation arbitrarily far from equilibrium by observing a relaxation process in Fock space. In Fig. 1 (a), the time evolution of the uncertainty function  $A$  is plotted. We set  $M = 1$  for all figures. For a state initially in a pure state, the uncertainty at  $t > 0$  is always greater than the initial value.

Since decoupling pulses will reduce or eliminate system-environment interaction and suppress the information loss in the system, the uncertainty can be used as a measure of the suppression of the environment-induced effect. In particular, after the application of sufficiently strong and frequent pulses, we expect that the states will obey an uncertainty relation

close to the initial relation, when the environment is almost completely decoupled from the system.

In Fig. 1 (b), the uncertainty function at  $t = 1$  is plotted as a function of the pulse frequency parameter  $\eta \equiv \Lambda_{UV}\Delta t/\pi$ . Note that arbitrary pulses do not always suppress the uncertainty. For slow pulses, the uncertainty is increased rather than decreased. The peak around  $\eta \sim 1$  is ascribed to the resonance between the pulse and the environmental mode. For super-Ohmic environment, the resonance is particularly eminent, while for  $1/f$  environment, the resonance is absent and the suppression of uncertainty is effective throughout the whole range of the pulse frequency in the figure. This phenomenon is related to so called quantum anti-Zeno effect. We will discuss this issue in Sec. 3.3. For pulses faster than the resonance  $\eta < 1$ , the uncertainty function decreases as the pulses become faster and for sufficiently fast pulses, the initial uncertainty returns for all environments.

### 3.3 Dynamical Decoupling in ESBM

In [23], it was shown that the bang-bang pulses with their pulse duration close to but less than the threshold value  $\pi/\Lambda_{UV}$  can eliminate  $1/f$  noises efficiently. A pure dephasing type model[29] was used to illustrate the case as follows. In the presence of the decoupling pulses, at  $t_{2N} = 2N\Delta t$ , coherence between the two levels is given in the interaction representation by

$$\rho_{01}^I(t_{2N}) = e^{-D_P(t_{2N})} \rho_{01}^I(0), \quad (58)$$

where

$$D_P(t_{2N}) \sim \int_{\Lambda_0}^{\Lambda_{UV}} d\omega I(\omega) \coth\left(\frac{\beta\omega}{2}\right) \frac{1 - \cos\omega t_{2N}}{\omega^2} \tan^2\left(\frac{\omega\Delta t}{2}\right) \quad (59)$$

The  $\tan^2$  factor contains the effect of decoupling pulses. This form indicates that decoherence will be suppressed for

$$\Lambda_{UV}\Delta t < \pi. \quad (60)$$

Indeed decoherence from all the modes with  $(4l + 1)\pi/2 < \omega\Delta t < (4l + 3)\pi/2$  for an integer  $l$  will be enhanced. There is also a resonance of decoupling pulses when the pulses are synchronized with the particular mode in an environment causing a divergence in the decoherence rate that leads to rapid destruction of coherence. Bang-bang method suppresses  $1/f$  noise for sufficiently fast pulses, but the condition (2) still needs to be satisfied.

At a finite temperature when thermal fluctuations begin to affect the system dynamics, a time scale  $t_{thermal}$  sets an additional constraint for decoupling. In order for the decoupling to be successful, the pulse interval needs to be smaller than the smaller value of  $1/\Lambda_{UV}$  or  $t_{thermal}$ [15].

Here we will show that this resonance effect does not appear in more realistic ESBM models.  $t_{environment}$  is not just a function of  $\Lambda_{UV}$  but depends on detailed characteristics

of the environment. In the case of our ESBM,  $t_{environment}$  also sensitively depends on the spectral density. In more general cases, there are many more parameters to determine  $t_{environment}$ , which should be determined by the spectroscopy of the environment.

Fig. 2 shows the time evolution of the logarithm of the decay factor  $\Gamma(t) \equiv -\log P_1$  at  $T = 0$  for different environments. Sufficiently fast pulses are chosen so that the decay rate is suppressed by the decoupling pulses. In the super-Ohmic case, the short time decay is remarkable due to ultra-violet mode dominance in this environment, while in the  $1/f$  case, long time decay is drastic due to infrared mode abundance in this environment. The efficiency of decoupling directly reflects this characteristic. In the super-Ohmic case, the suppression of decay rate is relatively small, while in the  $1/f$  case, improvement is rather remarkable.

In order to quantify how slow the pulses can be, let us introduce the parameter  $\eta \equiv \Lambda_{UV}\Delta t/\pi$ .  $\eta < 1$  means that the pulses for efficient suppression of decoherence in this environment need to be fast compared to the UV cutoff. This condition is difficult to be met experimentally.  $\eta > 1$  means that the pulses can be reasonably slow and relatively easy to implement. For  $1/f$  noise, where  $\eta = 1.5 > 1$ , our DD scheme works very well. For Ohmic environment,  $\eta = 0.15 \ll 1$ , and for super-Ohmic environment,  $\eta = 0.05 \ll 1$ , thus the pulses to suppress Ohmic and super-Ohmic environment need to be ultra-fast. We see that super-Ohmic environments can pose a serious obstacle for the implementation of coherent quantum operations.

In Fig. 3 (a), coherence as a function of the pulse interval is plotted in the pure-dephasing case. For super-Ohmic case, the suppression is the smallest and the condition for efficient suppression is much more stringent than  $\Lambda_{UV}\Delta t < \pi$ , while for  $1/f$  noise, the pulses with  $\Delta t$  close to  $\pi/\Lambda_{UV}$  remain effective. However, irrespective of the environment, when the pulse interval gets longer,  $\Lambda_{UV}\Delta t \sim \pi$ , there is a crossover from decoherence suppression to decoherence accentuation. There is a sharp resonance point at  $\Lambda_{UV}\Delta t = \pi$ , where decoherence rate diverges for all environment and the condition  $\Lambda_{UV}\Delta t < \pi$  need be strictly enforced.

In Fig. 3 (b), the effect of decoupling pulses in Eq. (10) is studied in our ESBM. The main difference from Fig. 2 (a) is that: (i) there is no sharp resonance as seen in Fig. 3 (a) in any environment although the crossover from decoherence suppression to accentuation can still be seen. (ii) the condition  $\Lambda_{UV}\Delta t < \pi$  is not necessary for the suppression of  $1/f$  noise. Even very slow pulses  $\Lambda_{UV}\Delta t \gg \pi$  can suppress it. The second condition (ii) expressed before in Eq. (2) is particularly important in that it is often too stringent for practical implementation with qubits. Note that the crossover behavior expressed in (i) is already manifest in the uncertainty relation plotted in Fig. 1(b). Similar effect also appears in the study of quantum Zeno effect where sufficiently frequent measurements suppress the population decay[33]. When the measurement is performed less frequently, there is a crossover from quantum Zeno effect to the so called quantum anti-Zeno effect, where measurement accelerates the decay[26].

### 3.4 Strong, long and slow pulse limit

We now study the limit of long ( $\tau \rightarrow \infty$ ) and slow ( $\Delta t \rightarrow \infty$ ) pulses, opposite to the cases considered so far. In this limit, the pulse Hamiltonian can be written as the interaction between the system Hamiltonian and the constant field:

$$H_P \rightarrow H_S V. \quad (61)$$

Let us consider the time evolution operator acting on the eigenstate of the total Hamiltonian:

$$U(t)|N\rangle = e^{-iE_N t}|N\rangle, \quad (62)$$

where  $H|N\rangle = E_N|N\rangle$ . We take the large  $V$  limit and consider the first order correction with respect to  $V^{-1}$ . Using the nondegenerate perturbation theory, we see that  $|N\rangle = |n\rangle + V^{-1}|n\rangle^{(correction)}$ ,  $E_N = V\epsilon_n + \langle n|H_S + H_I + H_E|n\rangle + O(V^{-1})$ , where  $|n\rangle$  and  $\epsilon_n = \Omega n$  are eigenstates and eigenvalues of the Hamiltonian  $H_S$ . By expanding (62) around these unperturbed states, we obtain in the large  $V$  limit,

$$\begin{aligned} U(t)|N\rangle &= e^{-iE_N t}|n\rangle + O(V^{-1}) \\ &= e^{-i(V\epsilon_n + \langle n|H_S + H_I + H_E|n\rangle + O(V^{-1}))t} + O(V^{-1}) \\ &= e^{-i((V+1)\epsilon_n + H_E)t} + O(V^{-1}) \end{aligned} \quad (63)$$

for all  $N$ . This implies

$$U(t) = e^{-i((V+1)H_S + H_E)t} + O(V^{-1}) \quad (64)$$

Thus in the limit of large  $V$ , the system-bath interaction  $H_I$  is eliminated. This effect resembles the quantum Zeno effect[33] in which the decay is suppressed by frequent measurements. Indeed a parallel argument with the quantum Zeno effect case is possible (64) and one can show that there is no relaxation in this limit[34]. From (64)

$$\begin{aligned} \rho_{nn}(t) &= \langle n|\hat{\rho}(t)|n\rangle \\ &= \text{Tr} [U(t)\hat{\rho}(0)U^{-1}(t)|n\rangle\langle n|] \\ &= \text{Tr} [\hat{\rho}(0)|n\rangle\langle n|] = P_n(0). \end{aligned} \quad (65)$$

The difference here from the quantum Zeno effect in [33] caused by repeated measurements is that the time evolution of the system in this case is unitary. The effect of the external field in (61) is to slow down the decay process. It can in principle provide an alternative method to dynamical decoupling although  $V$  is often uncontrollable as it is fixed by the design and fluctuations of  $V$  induce an additional source of decoherence. In Fig. 4, the excited state population is plotted as a function of the strength of the constant external field  $V$ . For Ohmic and super-Ohmic cases, frequency renormalization (Ohmic) and frequency and



mass renormalization (super-Ohmic) terms are taken into account by introducing counter terms[35] before applying  $V$ . These terms dominant at ultra-short times are not suppressed by the constant field in (61) while they can be suppressed by the pulse decoupling (10) as we saw in Sec.3.2 and 3.3. In Fig. 4, the decay can be suppressed from coupling to constant large external field  $V$  after the renormalization although overall suppression is not so remarkable as decoupling by pulses. In pulse decoupling, the effect of the environmental mode with frequency  $\omega \ll 1/\Delta t$  is suppressed, while in the constant field case, for any finite  $V$ , all the environmental modes upto  $\omega \sim 1/t$  contribute to decoherence.

### 3.5 Conclusion

In this paper, we propose a dynamical decoupling scheme for error prevention or deterrence based on the effective spin-boson model we introduced recently. A train of decoupling pulses with alternating signs creates a fictitious instantaneous Hamiltonian evolution. Our analysis does not make any of the conventional approximations such as the Born, Born-Markov, RWA or adiabatic approximation, thus enabling us to probe the system dynamics in a much wider parameter regime including the low temperature, ultra-short time scale and strong external field conditions which are likely to be more relevant for quantum information processing. We studied this method in a general environment with Ohmic, super-Ohmic and  $1/f$  spectral density functions. In all cases, in our decoupling scheme, there is no saturation of decoherence rate due to resonance as reported in previous studies using bang-bang controls. We saw the smooth crossover from suppression to accentuation of decoherence in our model that extends in a wide range of pulse durations. In particular, our method can suppress  $1/f$  noise with much slower pulses than previously studied. Due to the shielding of high energy modes in the environment as a result of defect motion, decoherence caused by telegraph noise is weaker at short times than that by  $1/f$  noise from the harmonic environment discussed in this paper. Thus we expect our pulse decoupling method could also provide efficient suppression of telegraph type noises.

For efficient suppression of decoherence from an Ohmic environment, the pulse parameter needs to satisfy  $\eta < 1$  and the pulses need to be fast compared to the UV cutoff, which is difficult to implement. For  $1/f$  noise,  $\eta > 1$ , thus the pulses can be reasonably slow and our scheme is relatively easy to implement. However, for super-Ohmic environment,  $\eta \ll 1$  and the pulses need to be ultra-fast. Thus the most serious obstacle for the implementation of quantum computing may be the presence of super-Ohmic environments.

We also studied the effect of strong constant field on the population decay. The decay process appears to slow down but the suppression is not so evident compared to the fast pulse decoupling.

In reality, we may not know enough information about the environment to identify the possible sources of decoherence [22]. But one can cleverly reverse the argument here and propose to use our decoupling method to obtain information about the environment spectrum by measuring the decoherence rate with changing pulse intervals. For instance, if the value of  $\eta$  at which the crossover between decoherence suppression and accentuation occurs is greater

than 1, the environment has sub-Ohmic spectrum. If smaller than 1, super-Ohmic.

At this point, we are not aware of any experimental results on super-Ohmic environments. Since an electromagnetic field seen by a charged electron due to charge-field interaction in a three dimensional space is a super-Ohmic environment[36] we expect this type of environment to be rather ubiquitous than peculiar. While the  $1/f$  noise due to charge-fluctuations in Coulomb forces are frequently observed and more dominant, super-Ohmic noise due to charge-photon interaction is likely to coexist with  $1/f$  noise. However, the short time dominant characteristics of super-Ohmic noise will make the actual detection very difficult.

In quantum computation with multiqubits, the entanglement among qubits is used as a resource for the speed-up of computation based on quantum algorithm. In the presence of entangling operation, the propagation of error in the whole computing space is unavoidable. To overcome this, fault tolerance is required in quantum error correction schemes[37]. The spreading of non-Markovian noise, in particular, noise of the super-Ohmic type in the computation architecture can be a serious threat to many proposed fault-tolerant computation schemes [38].

Our results are readily applicable to the study of quantum aspects in nanomechanical resonators[39] for which the system is commonly treated as a harmonic oscillator. ESBM[4] captures the essential short time dynamics common in many qubit models, in which their computational Hilbert space is obtained by the lowest two levels of the underlying multi-level structure. It also allows us to calculate the precise non-Markovian time evolution of leakage. The leakage is commonly neglected or crudely estimated in most of the popular theoretical models. Another application of our work is to superconducting Josephson junction qubits[40, 41, 42], in particular, the phase qubit models[43].

## Acknowledgments

This work is supported in part by a NSF-IRT grant PHY-0426696 and an ARDA contract MDA90401/C0903.

## References

- [1] *Decoherence and the Appearance of the Classical World in Quantum Theory*, eds. D. Giulini, *et al.* (Springer, Berlin, 1996).
- [2] J. P. Paz and W. H. Zurek, in *Coherent Matter Waves*, Les Houches Lectures Session LII, (North Holland, Amsterdam, 1999). W. H. Zurek *Rev. Mod. Phys.* **75**, 715-775 (2003).
- [3] M. A. Nielsen and I. L. Chuang, *Quantum Computation and Quantum Information* (Cambridge University Press, Cambridge, 2000).
- [4] K. Shiokawa and B. L. Hu, *Phys. Rev. A* **70**, 062106 (2004).
- [5] A. O. Caldeira and A. J. Leggett, *Physica A* **121**, 587 (1983); V. Hakim and V. Ambegaokar, *Phys. Rev. A* **32**, 423 (1985); F. Haake and R. Reibold, *Phys. Rev. A* **32**, 2462 (1985); H. Grabert, P. Schramm and G. L. Ingold, *Phys. Rep.* **168**, 115 (1988); W. G. Unruh and W. H. Zurek, *Phys. Rev. D* **40**, 1071 (1989); B. L. Hu, J. P. Paz and Y. Zhang, *Phys. Rev. D* **45**, 2843 (1992); *D* **47**, 1576 (1993).
- [6] B. L. Hu and Y. Zhang, *Mod. Phys. Lett. A* **8**, 3575 (1993); *Int. J. Mod. Phys. A* **10** (1995) 4537; J. J. Halliwell and A. Zoupas, *Phys. Rev. D* **52**, 7294 (1995); C. Anastopoulos and J. J. Halliwell, *Phys. Rev. D* **51**, 6870 (1995).
- [7] A. J. Leggett, S. Chakravarty, A. T. Dorsey, M. P. A. Fisher, A. Garg, and W. Zwerger, *Rev. Mod. Phys.* **59**, 1 (1987).
- [8] U. Weiss, *Quantum Dissipative Systems* (World Scientific, Singapore, 1999).
- [9] G.M. Palma, K.-A. Suominen and A. K. Ekert, *Proc. Roy. Soc. London Ser. A* **452**, 1996; P. Zanardi and M. Rasetti, *Phys. Rev. Lett.* **79**, 3306, (1997); L.-M. Duan and G. Guo, *Phys. Rev. A* **57**, 737 (1998); D. A. Lidar, I. Chuag, and B. Whaley, *Phys. Rev. Lett.* **81**, 2594, (1998).
- [10] M. Ban, *Jour. Mod. Opt.* **45**, 2315 (1998).
- [11] L. Viola and S. Lloyd, *Phys. Rev. A* **58**, 2733, (1998).
- [12] L. Viola, E. Knill, and S. Lloyd, *Phys. Rev. Lett.* **82**, 2417, (1999).
- [13] L.-M. Duan and G. Guo, *Phys. Lett. A* **261**, 139 (1999).
- [14] P. Zanardi, *Phys. Lett. A* **258**, 77 (1999).
- [15] D. Vitali and P. Tombesi, *Phys. Rev. A* **59**, 4178 (1999); *ibid* **65**, 012305 (2002).
- [16] C. Uchiyama, M. Aihara, *Phys. Rev. A* **66**, 032313, (2002).

- [17] D.A. Lidar and L.-A. Wu, Phys. Rev. A, **67**, 032313 (2003).
- [18] M. Byrd, L.-A. Wu, and D.A. Lidar, Jour. Mod. Opt. **51**, 2449 (2004).
- [19] G.S. Agarwal, M.O. Scully, and H. Walther, Phys. Rev. Lett. **86**, 4271, (2001).
- [20] C. Search and P.R. Berman, Phys. Rev. Lett. **85**, 2272 (2000).
- [21] A. G. Kofman and G. Kurizki, Phys. Rev. Lett., **87**, 270405 (2001).
- [22] M. Riebe, H. Haffner, C. F. Roos, W. Hänsel, J. Benheim, G. P. T. Lancaster, T. W. Körber, C. Becher, F. Schmidt-Kaler, D. F. V. James, and R. Blatt, Nature **429**, 734 (2004). M. Barrett, J. Chiaverini, T. Schaetz, J. Britton, W. M. Itano, J. D. Jost, E. Knill, C. Langer, D. Leibfried, R. Ozeri, and D. J. Wineland, Nature **429**, 737 (2004).
- [23] K. Shiokawa and D. A. Lidar, Phys. Rev. A **69**, 030302 (2004).
- [24] *Noise in Physical Systems and 1/f fluctuations*, edited by G. Bosman, (World Scientific, Singapore, 2001).
- [25] H. Gutmann, F. K. Wilhelm, W. M. Kaminsky, and S. Lloyd, Quantum Information Processing **3**, 247 (2004); L. Faoro and L. Viola, Phys. Rev. Lett., **92**, 117905 (2004); G. Falci, A. D'Arrigo, A. Mastellone, and E. Paladino, Phys. Rev. A **70**, R40101 (2004).
- [26] A. G. Kofman and G. Kurizki, Nature, **405**, 546 (2000).
- [27] E. Paladino, L. Faoro, G. Falci, and R. Fazio, Phys. Rev. Lett. **88**, 228304 (2002).
- [28] Y. Nakamura, Yu. A. Pashkin, T. Yamamoto, and J.S. Tsai, Phys. Rev. Lett. **88**, 047901 (2002).
- [29] W.G. Unruh, Phys. Rev. A **51**, 992 (1995).
- [30] E. Wigner, Phys. Rev. **40**, 749 (1932).
- [31] W. H. Luiselle, *Quantum Statistical Properties of Radiation* (Wiley, New York, 1990); L. Mandel and E. Wolf, *Optical Coherence and Quantum Optics* (Cambridge University Press, Cambridge, 1995); D. Walls and G. J. Milburn, *Quantum Optics* (Springer, Berlin, 1995); H. J. Carmichael, *Statistical Methods in Quantum Optics* (Springer, Berlin, 1999).
- [32] W. Heisenberg, Zeitschrift für Physik, **43** (1927).
- [33] B. Misra and E. C. G. Sudarshan, J. Math. Phys. **18**, 756 (1977).
- [34] P. Facchi and S. Pascazio, Phys. Rev. Lett. **89**, 080401-1 (2002).
- [35] K. Shiokawa and R. Kapral, J. Chem. Phys. **117**, 7852 (2002).

- [36] P. M. V. B. Barone and A. O. Caldeira, Phys. Rev. A **43**, 57 (1991). B. L. Hu and A. Matacz, Phys. Rev. D **49**, 6612 (1994).
- [37] P. Shor, in *Proceedings of the 37th Symposium on the Foundations of Computer Science*, Los Alamitos, California, 1996, IEEE press.
- [38] R. Alicki, M. Horodecki, P. Horodecki, and R. Horodecki, Phys. Rev. A **65**, 062101 (2002).
- [39] A.N. Cleland and M.L. Roukes, Appl. Phys. Lett. **69**, 2653 (1996); A. D. Armour, M. P. Blencowe, and K. C. Schwab, Phys. Rev. Lett. **88**, 148301 (2002).
- [40] Y. Makhlin, G. Schön, and A. Shnirman, Chem. Phys. **296**, 315 (2003).
- [41] D. Vion, A. Aassime, A. Cottet, P. Joyez, H. Pothier, C. Urbina, D. Esteve, M. H. Devoret, Science **296**, 886 (2002).
- [42] I. Chiorescu, Y. Nakamura, C. H. P. M. Harmans, and J. E. Mooij, Science **299**, 1869 (2003).
- [43] Y. Yu, S. Han, X. Chu, S. I. Chu, and Z. Wang, Science **296**, 8898 (2002); J. M. Martines, S. Nam, J. Aumentado, and C. Urbina, Phys. Rev. Lett. **89**, 117901-1 (2002); A. J. Berkley, H. Xu, R. C. Ramos, M. A. Gubrud, F. W. Strauch, P. R. Johnson, J. R. Anderson, A. J. Dragt, C. J. Lobb, and F. C. Wellstood, Science **300**, 1548.

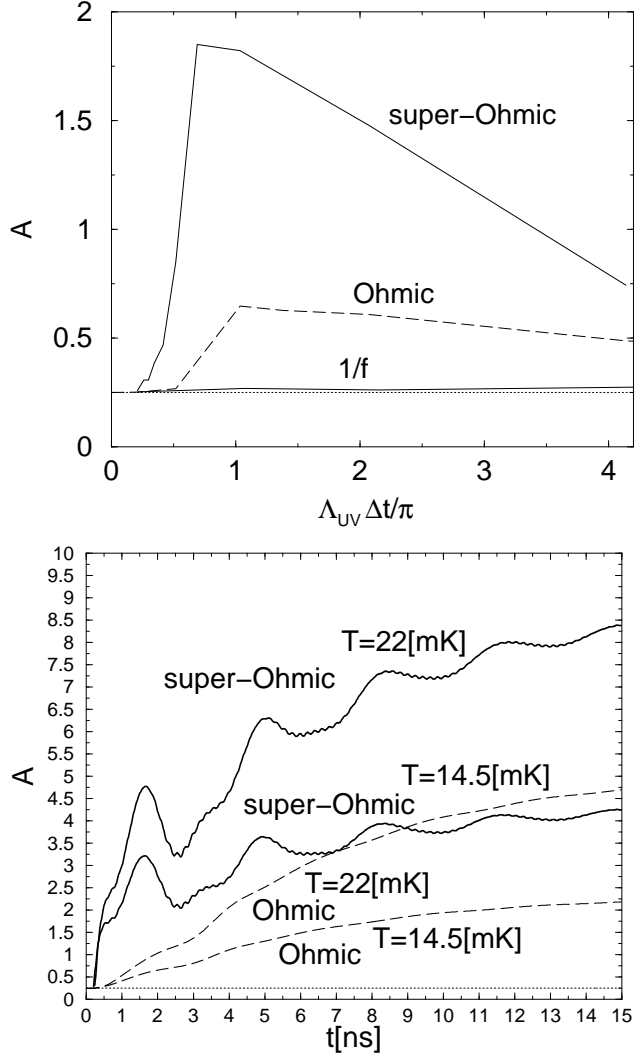


Figure 1: (a) The exact temporal evolution of the uncertainty function (56) in units of  $\hbar^2$  of a system initially in its ground state interacting with an Ohmic and super-Ohmic environment is plotted. The dotted line indicates the minimum uncertainty at  $1/4$ . All the curves start off from this value at  $t = 0$  [ns] and stay above the line. The effect of vacuum fluctuations of the environment sets in at  $t \sim 0.1$  [ns] and the effect of thermal fluctuations of the environment at  $t \sim 1/T = 0.3 - 0.5$  [ns] for Ohmic case. Both effects set in earlier for super-Ohmic case. Other parameters are  $\omega = 1$  [GHz],  $\gamma = 0.1$  [GHz],  $\Lambda_{UV} = 10$  [GHz]. (b) Same system now in the presence of decoupling pulses at  $t = 0.25$  [ns]. Other parameters are  $\Omega = 1$  [GHz].  $T = 14.5$  [mK],  $\gamma = 0.1$  [GHz],  $\Lambda_{UV} = 100$  [GHz] for Ohmic,  $T = 14.5$  [mK],  $\gamma = 0.0002$  [GHz],  $\Lambda_{UV} = 50$  [GHz] for super-Ohmic,  $T = 0$  [mK],  $\gamma = 0.1$  [GHz],  $\Lambda_{UV} = 100$  [GHz] for  $1/f$  environments.

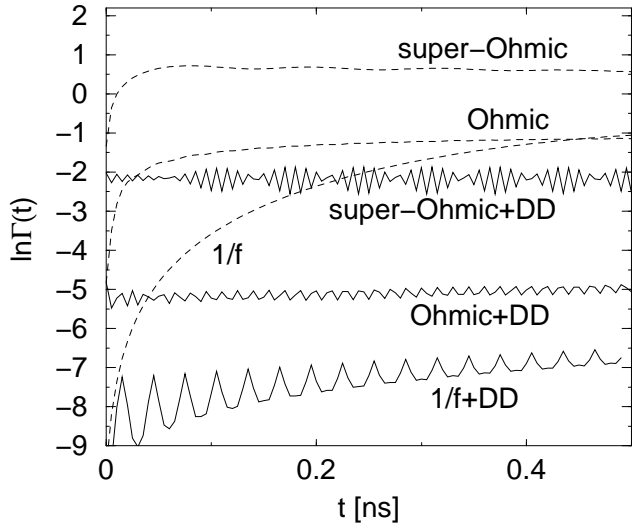


Figure 2: Plots of the logarithm of the decay factor at  $T = 0$ ,  $\Omega = 1[GHz]$ . Solid (Dashed) curves are decay with (without) decoupling pulses. Parameter values are:  $\Lambda_{UV} = 100[GHz]$ ,  $\gamma = 0.1[GHz]$ ,  $N = 100$  for Ohmic, and  $\Lambda_{UV} = 100[GHz]$ ,  $\gamma = 0.5[GHz]$ ,  $N = 30$  for 1/f,  $\Lambda_{UV} = 30[GHz]$ ,  $\gamma = 0.01[GHz]$ ,  $N = 100$  for super-Ohmic case.

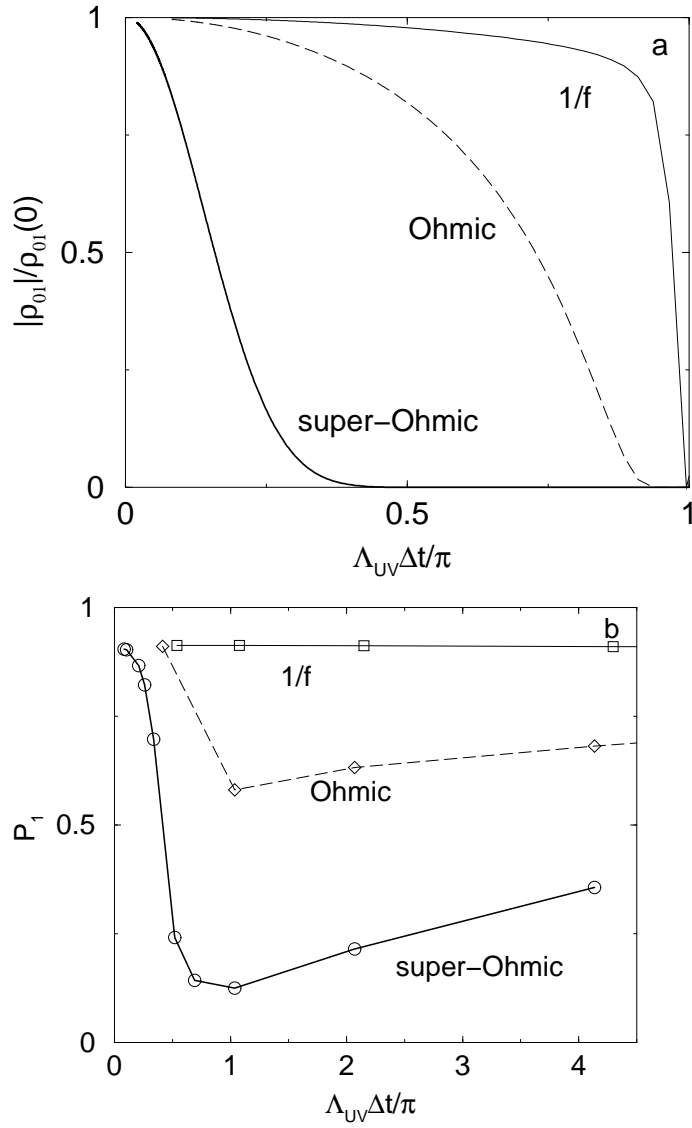


Figure 3: (a) Coherence as a function of the pulse interval at  $T = 0$  is plotted.  $t = 0.25[ns]$ . Parameters are:  $\Lambda_{UV} = 100[GHz]$ ,  $\Lambda_{IR} = 1$ .  $\gamma = 0.2[GHz]$  for 1/f,  $\gamma = 0.125[GHz]$  for Ohmic, and  $\gamma = 0.005[GHz]$  for super-Ohmic case. (b) Plots of the first excited state population at  $T = 0$  and  $t = 0.15[ns]$ . Other parameter values are:  $\Lambda_{UV} = 100[GHz]$ ,  $\Omega = 10[GHz]$ ,  $\gamma = 0.1[GHz]$  for Ohmic, and  $\Lambda_{UV} = 100[GHz]$ ,  $\Omega = 15[GHz]$ ,  $\gamma = 0.5[GHz]$  for 1/f,  $\Lambda_{UV} = 50[GHz]$ ,  $\Omega = 15[GHz]$ ,  $\gamma = 0.01[GHz]$  for super-Ohmic case. Parameter values are chosen to fit all the curves in the parameter range in the figure. For the same parameter values, while their qualitative behavior remains similar, the differences in their values are more striking.



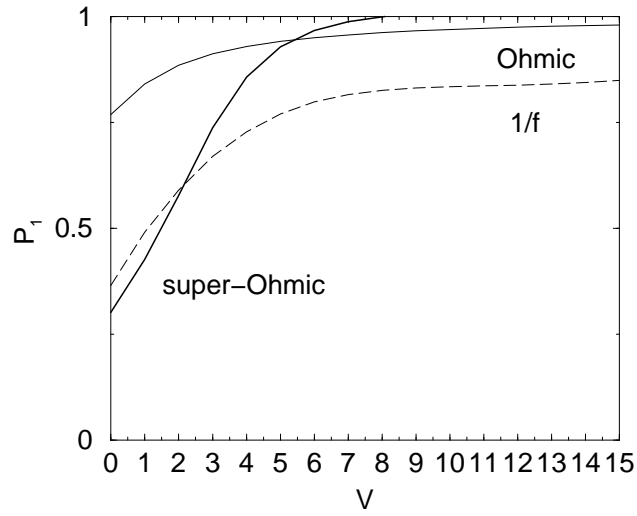


Figure 4: Excited state population as a function of  $V$  is plotted at  $t = 0.15[ns]$ . The initial state is the first excited state.  $\Lambda_{UV} = 100[GHz]$ .  $\Omega = 1[GHz]$ . Parameter values are:  $\gamma = 0.1[GHz]$  for Ohmic, and  $\gamma = 0.1[GHz]$  for 1/f,  $\gamma = 0.001[GHz]$  for super-Ohmic case.